

GW method applied to localized 4f electron systems

Athanasiос N. Chantis, Mark van Schilfgaarde and Takao Kotani¹

¹*School of Materials, Arizona State University, Tempe, Arizona, 85287-6006, USA*

(Dated: April 6, 2018)

We apply a recently developed quasiparticle self-consistent *GW* method (QSGW) to Gd, GdAs, GdN and ErAs. We show that QSGW combines advantages separately found in conventional *GW* and LDA+*U* theory, in a simple and fully *ab initio* way. QSGW reproduces the experimental occupied 4f levels well, though unoccupied levels are systematically overestimated. Properties of the Fermi surface responsible for electronic properties are in good agreement with available experimental data. GdN is predicted to be very near a critical point of a first-order metal-insulator transition.

PACS numbers: 71.15-m, 71.10-w, 71.20-Eh

Most 4f compounds belong to a class of materials whose electronic structure can be approximately described in terms of the coexistence of two subsystems — a localized *f* subsystem, and an itinerant *spd* subsystem. States near the Fermi energy E_F predominantly consist of the latter; 4f electrons largely play a passive role except to spin-polarize the *spd* subsystem through an indirect exchange mechanism. Describing both subsystems in the framework of *ab initio* electronic structure methods, however, poses a rather formidable challenge. The most widely used method, the local density approximation (LDA), has been an immensely successful tool that reasonably predicts ground-state properties of weakly correlated systems. The LDA is much less successful at predicting optical properties of such systems, and its failures become serious when correlations become moderately strong. It fails catastrophically for open *f*-shell systems, leaving *f* electrons at E_F . To surmount these failures, a variety of strategies to extend the LDA have been developed. These include exact exchange (EXX) [1], self-interaction-correction [2] (SIC), LDA+*U* [3, 4, 5], and more recently LDA+DMFT (dynamical mean-field theory) [6]. As a consequence, they have serious problems, both formal and practical. SIC, LDA+*U* and LDA+DMFT add nonlocal potentials to certain localized electrons in a special manner, leaving some ambiguity about how a localized electron state is defined, and how the double-counting term should be subtracted. Further, such approaches are specialized; they cannot remedy the LDA’s inadequate description of itinerant *spd* subsystems (e.g. its well-known underestimate of semiconductor bandgaps), which is the relevant one for transport properties. Thus, they are problematic for 4f materials such as the rare earth monopnictides we study here. The standard *GW* (i.e. 1-shot *GW* as perturbation to the LDA, or $G^{\text{LDA}}W^{\text{LDA}}$) significantly improves on the LDA’s description of itinerant *spd* subsystems, but it has many shortcomings [7]; and it fails qualitatively in open *f* systems, in much the same way as the LDA fails [7].

In short, the present status consists of an unsatisfactory patchwork of methods, each with successes in im-

proving some property in one or another class of materials. Here we show, for the first time, that a recently developed quasiparticle self-consistent *GW* method [8, 9, 10, 11] (QSGW) can reliably describe open *f*-shell systems, including the *spd* subsystem. The *GW* approximation is a prescription for mapping the non-interacting Green function to the dressed one, $G^0 \rightarrow G$. Formally, G can be calculated from any G^0 . QSGW gives a prescription to specify a (nearly) optimal mapping $G \rightarrow G^0$, so that $G^0 \rightarrow G \rightarrow G^0 \rightarrow \dots$ can be iterated to self-consistency. At self-consistency the quasiparticle energies of G^0 coincide with those of G . Thus QSGW is a self-consistent perturbation theory, where the self-consistency condition is constructed to minimize the size of the perturbation. QSGW is parameter-free, independent of basis set and of the LDA [11]. It contains LDA+*U* kinds of effects, but no subsystem is singled out for specialized treatment; there are no ambiguities in double-counting terms, or in what is included and what is left out of the theory. We showed that QSGW reliably describes a wide range of *spd* systems [9]. Its success in describing *f* systems is important because it is not known whether the *GW* method can reasonably describe correlated *f* electrons at all.

In addition, this work brings out some new fundamental points. First, the position of unoccupied *f* levels is systematically overestimated. Second, we predict that GdN is on the cusp of a new kind of first-order metal-insulator transition (MIT). Last, we show that the shifts in *f* levels that QSGW determines relative to LDA, lie outside the degrees of freedom inherent in the standard LDA+*U* method. The method enables us to reconstruct parameters used in the LDA+*U* theory, as we will show.

Ref. [11] gives some formal justification as to why QSGW should be preferred to conventional self-consistent *GW*. The orbital basis and our development of the all-electron *GW* are described in Ref. [7]. Local orbitals (e.g. 5f states) are essential for reliable description of these systems in QSGW. It is also important not to assume time-reversal symmetry in the open *f* systems [12].

We considered the following 4f systems: Gd, Er, EuN, GdN, ErAs, YbN, and GdAs. Gd and Er are metals,

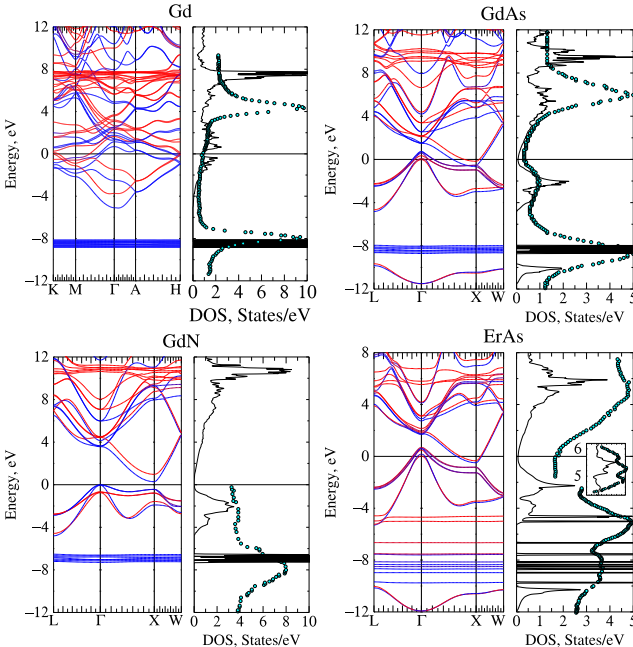


FIG. 1: The QSGW energy band structure of Gd, GdAs, GdN, and ErAs. Right panels show DOS, together with experimental XPS and BIS data[4, 13, 14, 15] (circles). $E_F=0$ eV. Colors indicate the spin character of the band (blue for majority and red for minority). Lattice constants were taken to be 5.00 Å (GdN), 5.80 Å (GdAs), 5.73 Å (ErAs) in the NaCl structure, and 3.64 Å (Gd) in hcp.

while the rest are narrow-gap insulators or semimetals. QSGW always shifts 4f levels away from E_F . The electronic structure around E_F is dominated by *spd* electrons, which we will consider later. Fig. 1 shows energy bands and QP density of states (DOS), for some cases, together with XPS (X-ray photoemission) and BIS (bremsstrahlung isochromat) spectroscopies.

f subsystem: In all cases, stable ferromagnetic solutions were found with the 4f element in the 3+ state; that is 6, 7, 11, and 13 f levels are occupied in Eu, Gd, Er, and Yb, respectively; the remainder are unoccupied. (Antiferromagnetic solutions were also found, but FM solutions are presented here to compare with Shubnikov–de Haas (SdH) experiments.) Occupied 4f levels were always dispersionless, as Fig. 1 shows, while unoccupied states show some dispersion, reflecting their hybridization with the *spd* subsystem. Gd is the only 4f element for which the LDA and $G^{\text{LDA}}W^{\text{LDA}}$ do not put f states at E_F [18], because the majority $4f^\uparrow$ states are filled and minority $4f^\downarrow$ states are empty. The two are separated by an exchange splitting ($U-J$ in LDA+ U terminology). For the remaining 4f elements either the $4f^\uparrow$ or the $4f^\downarrow$ level is partially filled. QSGW predicts large exchange splittings *within* this channel (controlled by different combinations of U and J); see e.g. the ErAs DOS in Fig. 1. Occupied f levels are generally in reason-

TABLE I: QSGW spin and orbital moments (bohr), average position of 4f levels relative to E_F (eV), and corresponding peaks in XPS and BIS data (where available). When f^\downarrow or f^\uparrow states are split between occupied and unoccupied levels, average positions for both occupied and unoccupied are given (top and bottom numbers). When the occupied or unoccupied part of f^\downarrow or f^\uparrow levels consist of multiple states split about the average (see, e.g. ErAs bands in Fig. 1), the range of splitting is denoted in parentheses.

	μ_{spin}	μ_{orb}	μ_{exp}	f^\uparrow	XPS	f^\downarrow	BIS
Gd	7.8	—	7.6 ^a	-8.5	-8.0	7.7	4.2
Er	3.5	6.0	9.1 ^b	-8.1(2) 3.1	-8.4,-4.6 5.1	-4(1)	2.1
EuN	6.0	-2.8		-6(2) 3.1		9	
GdN	7.0	—		-8.3	-8.5	9.5	5.8
GdAs	7.0	—		-7.0	-8.0	10.7	6
ErAs	3.0	6.0		-8.5(2) -9,-4.8	-9,-4.8	-5 6	5
YbN	1.0	3.0		-7(1)	-6.5	-6 4.5	0.2

^aReference [16]

^bReference [17]

able agreement with available XPS data (see Table I). In the two Er compounds (Er and ErAs), occupied f^\uparrow and f^\downarrow levels are fairly well separated. The shallower $4f^\downarrow$ levels likely correspond to the XPS peak between -4.5 and -5 eV, and the $4f^\uparrow$ levels to the broad XPS peak between -8 and -10 eV shown in Fig. 1. In YbN, the separation between occupied f^\uparrow and f^\downarrow is small, and the XPS peak (whose width is \sim 3 eV) probably corresponds to some average of them. More precise identification is not possible because multiplet effects are not included. In contrast, the *unoccupied* 4f levels are systematically higher than observed BIS peaks, typically by \sim 3-4 eV. The only exception is ErAs, where the overestimate is closer to 1 eV. (This may well be an artifact of final-state effects in ErAs, as suggested in Ref. 4.)

Overall, the $4f^\uparrow$ - $4f^\downarrow$ splitting is 16.2 eV in Gd, and \sim 18 eV in GdN and GdAs. This *change* in the splitting is reflected in the BIS-XPS data (12.2 eV for Gd, 14 eV for GdN and GdAs). The carrier concentration at E_F is larger in Gd than in GdAs, which results in a larger dielectric response, and more strongly screened U .

The *orbital moments* follow what is expected from Hund's rule. The spin moments are a little overestimated in the metals Er and Gd, following the trend observed in 3d magnetic systems such as MnAs [9].

Deviations from experiment can be qualitatively explained as follows. QSGW overestimates unoccupied states in *sp* semiconductors by \sim 0.2 eV [9]. The overestimate is somewhat larger in itinerant TM oxides such as SrTiO₃ and TiO₂ (\lesssim 1 eV), and is larger still (\gtrsim 1 eV) in the correlated oxide NiO [8, 11]. This can be under-

stood as a neglect of electron-hole interactions (excitonic effects). Short-range, atomic-like excitations shift peaks in $\text{Im}\epsilon(\omega)$ to lower frequency, increase the screening and reduce the strength of W . It is to be expected that the more localized states are, the stronger electron-hole correlations will be ($4f > \text{localized } 3d > \text{itinerant } 3d > sp$). Indeed, when $\text{Im}\epsilon(\omega)$ is calculated through the Bethe-Salpeter equation, it is in dramatically better agreement with experiment in sp systems (see, e.g. Ref. 19). The expected corrections to W are consistent with the observed trends, both in the overestimate of unoccupied QPEs (increasing with localization), and the overestimate of magnetic moments. However, is also likely that vertex corrections to GW play an increasingly greater role as localization increases. It is beyond the scope of our ability to include either kind of vertex correction in QSGW at present.

The spd subsystem comprises the states at E_F , which control electronic transport properties. Table II presents two of the de Haas-van Alphen (dHvA) frequencies observed in Gd. By comparing them to the calculated ones as a function of E_F , we can determine the shift in E_F required to match the dHvA data [20], and thus assess the error in those bands at E_F . Table II shows that the QSGW γ_1 and α_1 should be shifted by ~ -0.2 eV and -0.1 eV, respectively, consistent with precision of QSGW for itinerant systems [9]. The QSGW DOS at E_F (1.84 states/eV·atom) is slightly overestimated (1.57 states/eV·atom [21]).

ErAs and GdAs may be viewed as slightly negative-gap insulators (semimetals), with an electron pocket at X compensated by a hole pocket at Γ (see Fig. 1). Several experiments address the spd subsystem near E_F :

(i) The As- p -like Γ_{15} band dispersion between Γ and X in ErAs. As seen in Fig. 1, the X point has states at -1.2 eV and -0.8 eV, and split-off bands at -3.52 eV. A single band from Γ to X of width ~ 1.5 eV was observed by photoemission (Fig. 7 of Ref. 4).

(ii) SdH frequencies f and cyclotron masses m^* (see Table III). SdH measurements in $\text{Er}_{0.68}\text{Sc}_{0.32}\text{As}$ [22] agree reasonably well with QSGW calculations for ErAs. Allen et al. [23] estimated $m^*=0.17$ from dc field measurements for ErScAs, which is consistent with the QSGW values $m^*(e_{\bar{A}\uparrow})=0.16$, $m^*(e_{\bar{A}\downarrow})=0.13$. Nakanishi et al. [24] identified two branches in the [100] direction from dHvA measurements in GdAs: $m^*=0.2$ ($f=246$ T) for

TABLE II: Gd dHvA Frequencies (T) for a magnetic field oriented along the [0001] direction. γ_1 originates from the majority $6s$ band and α_1 from the majority $5d$ band. Both lie in the ΓKM plane; they are depicted in Ref. [20].

	$E_F-0.2$ eV	$E_F-0.1$ eV	E_F	Expt [20]
α_1	4934	4260	3585	4000
γ_1	7209	6099	5177	6900

TABLE III: QSGW cyclotron masses m^* , in units of the free electron mass m , and frequencies f (Tesla) for GdAs and ErAs. Three bands cross E_F near Γ (see Fig. 1): the heavy hole ($h1$), light hole ($h2$) and split-off hole (sh). Ellipsoids at X have two inequivalent axes, $e_{\bar{B}C}$ and $e_{\bar{A}}$. Also shown are SdH frequencies measured for $\text{Er}_{0.68}\text{Sc}_{0.32}\text{As}$ [22]. Petukhov *et al.* showed that Sc doping has a modest effect on the Fermi surface, at least within the LDA(core-like $4f$) approximation [5]. $sh\uparrow$ and $sh\downarrow$ are not distinguished in experiments. Notation follows Ref. [22] except that \uparrow and \downarrow are exchanged.

	GdAs			ErAs	
	m^*/m	f (T)	m^*/m	f (T)	f (T)
$e_{\bar{A}\uparrow}$	0.17	392	0.16	452	386
$e_{\bar{A}\downarrow}$	0.15	95	0.13	301	328
$e_{\bar{B}C\uparrow}$	0.51	1589	0.49	1317	1111
$e_{\bar{B}C\downarrow}$	0.31	386	0.44	887	941
$h1\uparrow$	0.34	1575	0.43	1642	1273
$h1\downarrow$	0.40	1433	0.45	1368	1222
$h2\uparrow$	0.23	712	0.26	726	612
$h2\downarrow$	0.26	571	0.24	590	589
$sh\uparrow$	0.12	191	0.06	174	150
$sh\downarrow$	0.08	9	0.07	25	

$m^*(e_{\bar{A}})$, and $m^*=0.26$ ($f=439$ T) for $m^*(h_2)$. These are in good agreement with QSGW values in Table III. Koyama *et al.* [25] obtained $m^*=0.48$ from a broad peak in cyclotron experiments. This may be understood as some kind of average of masses in Table III.

(iii) The electron concentration in the pocket at X is controlled by the (negative) gap between Γ and X . The QSGW result agrees with experiment to within the reliability of the calculated bandgap (~ 0.2 eV):

ErAs: 3.5×10^{20} cm $^{-3}$ QSGW; 3 ± 1 expt, Ref [24]
GdAs: 3.3×10^{20} cm $^{-3}$ QSGW; 2.3 expt, Ref [26]

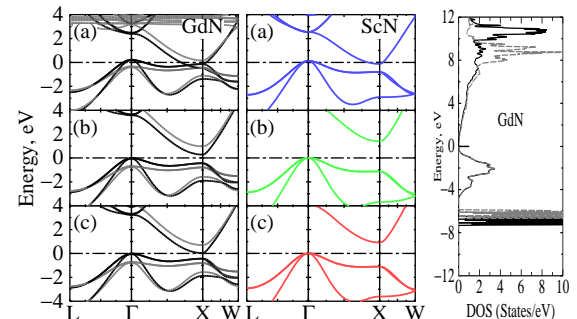


FIG. 2: Energy bands near E_F ($E_F=0$) in GdN and ScN. For GdN, majority (minority) bands are drawn in dark (light) lines. (a) LDA+ U for GdN ($U=6.7$ eV, $J=0.69$ eV) and LDA for ScN. A semimetal is predicted in both cases. (b) QSGW bands: both materials have positive gaps. (c) ‘scaled Σ ’ bands (see text). The ScN Γ - Γ and Γ - X gaps fall close to measured values ($E_c(X)-E_v(\Gamma)=0.9 \pm 0.1$ eV; $E_c(X)-E_v(X)=2.15$ eV [27]). Right panel: DOS in QSGW (dark lines) and ‘scaled Σ ’ (light lines). Scaling reduces the $4f^\downarrow$ - $4f^\uparrow$ splitting, but the spd subsystem is little affected by it.

GdN is qualitatively similar to GdAs and ErAs, but there is some confusion as to whether GdN is an insulator or semimetal. Wacher and Kaldis measured a large carrier concentration ($1.9 \times 10^{21} \text{ cm}^3$). But, direct measurements of resistivity indicate insulating behavior [28]. Remarkably, QSGW predicts *two kinds* of stable, self-consistent solutions near the observed lattice constant $a=5.00$: one is insulating with $E_g(a)=E_c(\text{X})-E_v(\Gamma)=+0.2 \text{ eV}$, and $\partial E_g/\partial a = 2.7 \text{ eV}/\text{\AA}$. It is stable for $a>4.96 \text{\AA}$. The other is a semimetal with $E_g(a)=-0.2 \text{ eV}$ and $\partial E_g/\partial a = 2.1 \text{ eV}/\text{\AA}$. It is stable for $a<4.99 \text{\AA}$ and at larger lattice constants when a tetragonal or trigonal shear is applied. Thus, a range of structures is found for which two solutions coexist, and the MIT is *first-order*. It can be connected with discontinuous changes in the dielectric function: $\epsilon(\omega \rightarrow 0)$ diverges in the semimetallic phase, and approaches a constant in the insulating phase.

To correct for QSGW's tendency to overestimate gaps slightly, we adopt the ‘scaled Σ ’ approach [10]: we take a linear combination of the LDA and the QSGW potentials, $(1-\alpha) \times \text{QSGW} + \alpha \times \text{LDA}$. We found that $\alpha=0.2$ can accurately reproduce experimental band gaps for a wide variety of materials; see Ref. 10 for III-V and II-VI semiconductors. Energy bands with $\alpha=0.2$ are shown in Fig. 2(c). For comparison, we also show the bands of ScN, whose electronic structure is similar to GdN near E_F . Scaling brings the ScN Γ -X and X-X gaps to within $\sim 0.1 \text{ eV}$ of experiment, consistent with our general experience. It is reasonable to expect that GdN will be similarly accurate. Panel (c) shows that for GdN, $E_g \approx 0.05 \text{ eV}$. Thus GdN is right on the cusp of a MIT. The spin-averaged X-X gap (1.48 eV for majority, and 0.46 eV for minority) is in close agreement with 0.98 eV measured in paramagnetic GdN [29].

Comparison between QSGW and LDA+U: In both methods, the one-particle effective potential is written as $V^{\text{eff}} = V^{\text{LDA}} + \Delta V$. In QSGW, ΔV is rather general; in LDA+U, ΔV is added only for the onsite ff block which is specified by U and J [30]. For comparison, we extract the onsite ff block (QSGW[$f-f$]) from V^{eff} given by QSGW, by Fourier transform techniques [11]. The *spd* subsystem near E_F almost perfectly recovers the LDA-like bands of the LDA+U method, Fig. 2(a); the f subsystem remains essentially unchanged from the full QSGW calculation, Fig. 1(c). Thus, the QSGW H_0 may be thought of as the “ultimate” LDA+U Hamiltonian, with Hubbard parameters connecting all orbitals between all sites in a basis-independent way. Significantly, *no choice* of the standard LDA+U parameters can reproduce the QSGW (f^\downarrow, f^\uparrow) levels simultaneously, because their average position is essentially determined from the LDA.

This work was supported by ONR contract N00014-02-1-1025. We are also indebted to the Ira A. Fulton High Performance Computing Initiative. A. N. Chantis would like to thank A. G. Petukhov for fruitful discussions.

- [1] T. Kotani, J.Phys.: Condens. Matter **10**, 9241 (1998).
- [2] C. M. Aerts, P. Strange, M. Horne, W. M. Temmerman, Z. Szotek, and A. Svane, Phys. Rev. B **69**, 045115 (2004).
- [3] C. gang Duan, R. F. Sabiryanov, J. Liu, W. N. Mei, P. A. Dowben, and J. R. Hardy, Phys. Rev. Lett. **94**, 237201 (2005).
- [4] T. Komesu, H.-K. Jeong, J. Choi, C. N. Borca, P. A. Dowben, A. G. Petukhov, B. D. Schultz, and C. J. Palmstrom, Phys. Rev. B **67**, 035104 (2003).
- [5] A. G. Petukhov, W. R. L. Lambrecht, and B. Segall, Phys. Rev. B **53**, 3646 (1996).
- [6] S. Y. Savrasov, K. Haule, and G. Kotliar, Phys. Rev. Lett. **96**, 036404 (2006).
- [7] M. van Schilfgaarde, T. Kotani, and S. V. Faleev, Phys. Rev. B **74**, 245125 (2006).
- [8] S. V. Faleev, M. van Schilfgaarde, and T. Kotani, Phys. Rev. Lett. **93**, 126406 (2004).
- [9] M. van Schilfgaarde, T. Kotani, and S. Faleev, Phys. Rev. Lett. **96**, 226402 (2006).
- [10] A. N. Chantis, M. van Schilfgaarde, and T. Kotani, Phys. Rev. Lett. **96**, 086405 (2006).
- [11] T. Kotani, M. van Schilfgaarde, and S. Faleev (2006), preprint <http://arxiv.org/abs/cond-mat/0611002>.
- [12] P. Larson, W. Lambrecht, and et al. (2006), in press, Phys. Rev. B (2007).
- [13] J. K. Lang, Y. Baer, and P. A. Cox, J. Phys. F: Metal Phys. **11**, 121 (1981).
- [14] H. Yamada, T. Fukawa, T. Muro, Y. Tanaka, S. Imada, S. Suga, D.-X. Li, and T. Suzuki, J. Phys. Soc. Jpn **65**, 1000 (1996).
- [15] F. Leuenberger, A. Parge, W. Felsch, K. Fauth, and M. Hessler, Phys. Rev. B **72**, 014427 (2005).
- [16] L. W. Roeland, G. J. Cock, F. A. Muller, A. C. Moleman, K. A. McEwen, R. G. Jordan, and D. W. Jones, J. Phys. F **5**, L233 (1975).
- [17] J. Jensen and A. R. Mackintosh, *Rare earth magnetism: structures and excitations* (Clarendon Press, Oxford, 1991).
- [18] F. Aryasetiawan and K. Karlsson, Phys. Rev. B **54**, 5353 (1996).
- [19] L. X. Benedict, E. L. Shirley, and R. B. Bohn, Phys. Rev. B **57**, 9385 (1998).
- [20] P. G. Mattocks and R. C. Young, J. Phys. F: Metal Phys. **7**, 1219 (1977).
- [21] P. Wells, P. C. Lanchester, D. W. Jones, and R. G. Jordan, J. Phys. F **4**, 1729 (1974).
- [22] R. Bogaerts, F. Herlach, A. D. Keyser, F. M. Peeters, F. DeRosa, C. J. Palmstrom, D. Brehmer, and J. S. J. Allen, Phys. Rev. B **53**, 15951 (1996).
- [23] J. S. J. Allen, F. DeRosa, C. J. Palmstrom, and A. Zrenner, Phys. Rev. B **43**, 9599 (1991).
- [24] Y. Nakanishi, F. Takahashi, T. Sakon, M. Yoshida, D. X. Li, T. Suzuki, and M. Motokawa, Physica B **281**, 750 (2000).
- [25] K. Koyama, M. Yoshida, T. Sakon, D. Li, T. Suzuki, and M. Motokawa, J. Phys. Soc. Jpn. **69**, 3425 (2000).
- [26] J. S. J. Allen, N. Tabatabaie, C. J. Palmstrom, G. W. Hull, T. Sands, F. DeRosa, H. L. Gilchrist, and K. C. Garrison, Phys. Rev. Lett. **62**, 2309 (1989).
- [27] H. A. Al-Brithen, A. R. Smith, and D. Gall, Phys. Rev. B **70**, 045303 (2004).

- [28] J. Q. Xiao and C. L. Chien, Phys. Rev. Lett. **76**, 1727 (1996).
- [29] E. Kaldis and C. Zurcher, Helv. Phys. Acta **47**, 421 (1974).
- [30] V. I. Anisimov, F. Aryasetiawan, and A. I. Lichtenstein, J. Phys.: Condens. Matter **9**, 767 (1997).

